Supporting Information

Graphitic Carbon Nitride Modified by Methyl Viologen and I_3^-/I^- carrier relay for Improved Photocatalytic Hydrogen Evolution

*Tania Tofaz, Jing-Han Li, Shuai Chen, Hao-Yang Ding, Ru-Xin Tian, and An-Wu Xu**

Division of Nanomaterials and Chemistry, Hefei National Research Center for Physical Sciences at the Microscale, University of Science and Technology of China, Hefei 230026, P. R. China.

Corresponding Author

*E-mail: anwuxu@ustc.edu.cn (A.W. X)

1. Characterizations

X-ray diffraction (XRD) patterns were collected on a Rigaku TTR-III diffractometer (MXPAHF, Japan) with Cu Kα irradiation (λ = 1.541 Å), operating voltage of 40 kV, and a current of 200 mA. Fourier-transform infrared spectroscopy (FT-IR) analysis of the samples with KBr pellets was carried out using a Nicolet Nexus 8700 FT-IR spectrometer. The UV-Vis diffuse reflectance spectra (UV-Vis DRS) of the photocatalysts were recorded using a Shimadzu 3700DUV spectrophotometer, scanning with a wavelength range from 300 nm to 800 nm. Transmission electron microscopy (TEM) images were obtained using a JEM-2100 Plus transmission electron microscope operated at 200 kV. The X-ray photoelectron (XPS) spectra and valence band X-ray photoelectron spectra (VB-XPS) were recorded on a Thermo ESCALAB 250Xi spectrometer with an excitation source of monochromatized Al Ka (hv = 1486.6 eV) and a pass energy of 30 eV. The values of binding energies were calibrated with the C *1s* peak of contaminant carbon at 284.80 eV. The steady-state photoluminescence (PL) measurement was conducted on a fluorescence spectrophotometer (JY Fluorolog-3-Tau) with the excitation wavelength at 365 nm. Scanning electron microscopy (SEM, JEOL SM–6601F), and HAADF–STEM with corresponding EDS elemental mapping (HAADF–STEM JEOL–2010) were employed to evaluate the surface properties of the as-made samples. Kelvin probe force microscopy (KPFM) was analyzed using a conductive probe (SCM-PIT V2) on an Atomic Force Microscope (AFM, Bruker) Dimension Icon with an atmospheric environment. The multiple-point Brunauer-Emmett-Teller (BET) procedure was used to obtain specific areas of the samples. A Bruker AVANCE III 400 MHz WB solid-state Nuclear Magnetic Resonance Spectrometer was used for NMR spectra, where the ^{13}C 90-degree pulse length was 3.19 us @ 100 W. The electron paramagnetic resonance (EPR) spectrum of the

samples was obtained by a Bruker model JEOL JES-FA200 ESR. Microwave power employed was 1 mW; sweep width ranged from 223 to 423 mT. Modulation frequency and modulation width were 100 kHz and mT, respectively.

2. Photoelectrochemical Measurements

The photoelectrochemical tests of the photocatalysts were measured at room temperature using a CHI 760E (Shanghai Chenhua Limited, China) electrochemical workstation based on a standard three-electrode system, that is made up of a saturated Ag/AgCl (in saturated KCl solution) as the reference electrode, a platinum wire as the counter electrode, a fluorine-doped tin oxide (FTO) glass deposited with the photocatalysts as the working electrode and Na_2SO_4 (0.5 M, 100 mL) as the electrolyte solution. To make a working electrode, 2 mg of catalysts were dispersed into 1 mL ethanol containing 10 μL Nafion (5 wt%, D520, DuPont Inc., USA) by ultrasonication. The resulting dispersion was then transferred onto a piece of FTO glass (an effective area of about 1.0 cm^2) using a spin-coating method and dried at 60 ℃ for 2 h in an oven to form the final electrode.

The transient photocurrent responses were tested for each switch on/off (300 W Xe lamp) event with a bias voltage of 0.5 V. The electrochemical impedance spectroscopy (EIS) curves were measured under visible light and a bias of -0.2 V to evaluate the charge-transfer ability of the catalysts, and its frequency ranging from 10 MHz to 100 KHz.

3. Photocatalytic Hydrogen Evolution Measurements

Photocatalytic H_2 evolution from water splitting was carried out in a Pyrex top-irradiation reaction vessel (500 mL) connected to a glass-closed gas circulation and evacuation system (Prefect Light, Beijing, Labsolar-6A). In a typical experiment, a 50 mg photocatalyst was dispersed in a 100 mL aqueous solution containing 10 vol% TEOA as a sacrificial reagent. Then, 1 wt% Pt was loaded onto the photocatalyst surface by photo-deposition of $H_2PtCl_6 \cdot 6H_2O$, serving as a co-catalyst. The suspension was evacuated several times to remove air and other gases completely, then irradiated by a 300 W Xenon lamp. An appropriate long-pass cut-off filter (λ ≥ 420 nm) was employed to remove UV light and achieve visible-light irradiation. Additionally, the Pyrex reactor with a double layer was continuously stirred during the photocatalytic reaction, and the temperature of the reaction solution was maintained at 6 °C by a flow of cooling water. The amount of hydrogen evolution from the photocatalytic splitting of water was analyzed by using an online gas chromatograph (GC1120, Shanghai Sunny Hengping Limited) with a thermal conductivity detector (TCD) and a capillary column (5 Å molecular sieve). High-purity nitrogen was used as a carrier gas. The photocatalytic reaction time for each experiment was set as 4 h.

The AQE of CN-KI_3-KI-MV 1% at different monochromatic lights (λ = 420, 450, 500, and 550 nm ± 5 nm) was calculated via the following equation:

$$AQE = \frac{number\ of\ evolved\ H_2\ molecules\ x\ 2}{incident\ photons\ number}\ x\ 100\%$$

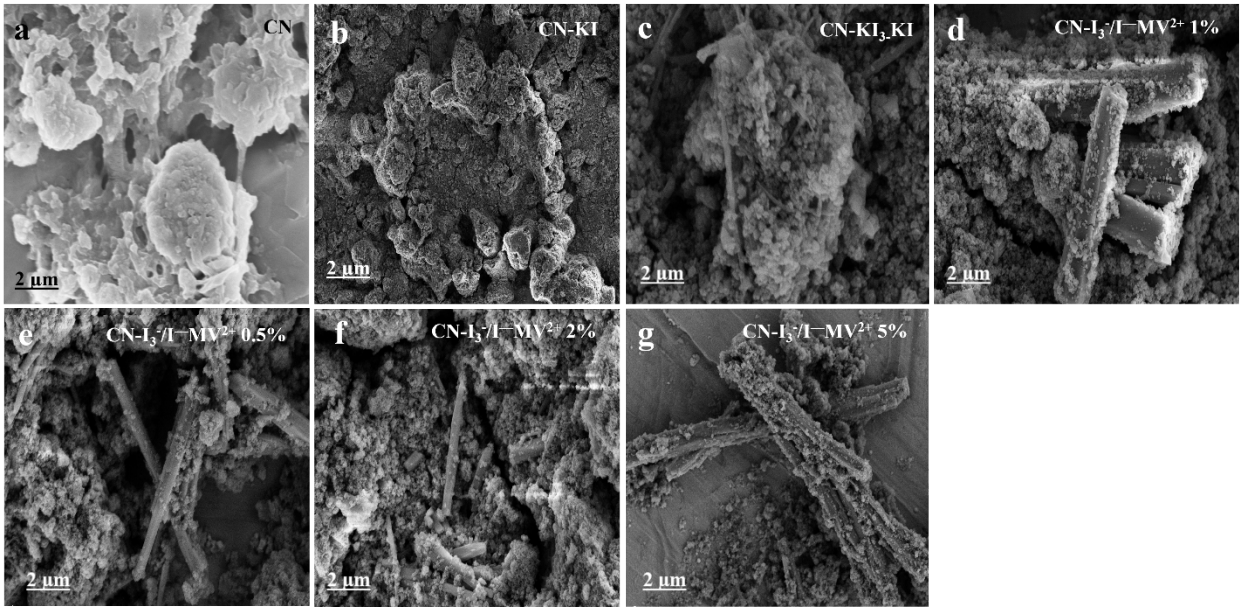

Fig. S1. SEM images of a) CN, b) CN-KI, c) CN-KI_3-KI, d) CN-I_3^-/I^--MV^{2+} 1%, e) CN-I_3^-/I^--MV^{2+} 0.5%, f) CN-I_3^-/I^--MV^{2+} 2%, and g) CN-I_3^-/I^--MV^{2+} 5% samples.

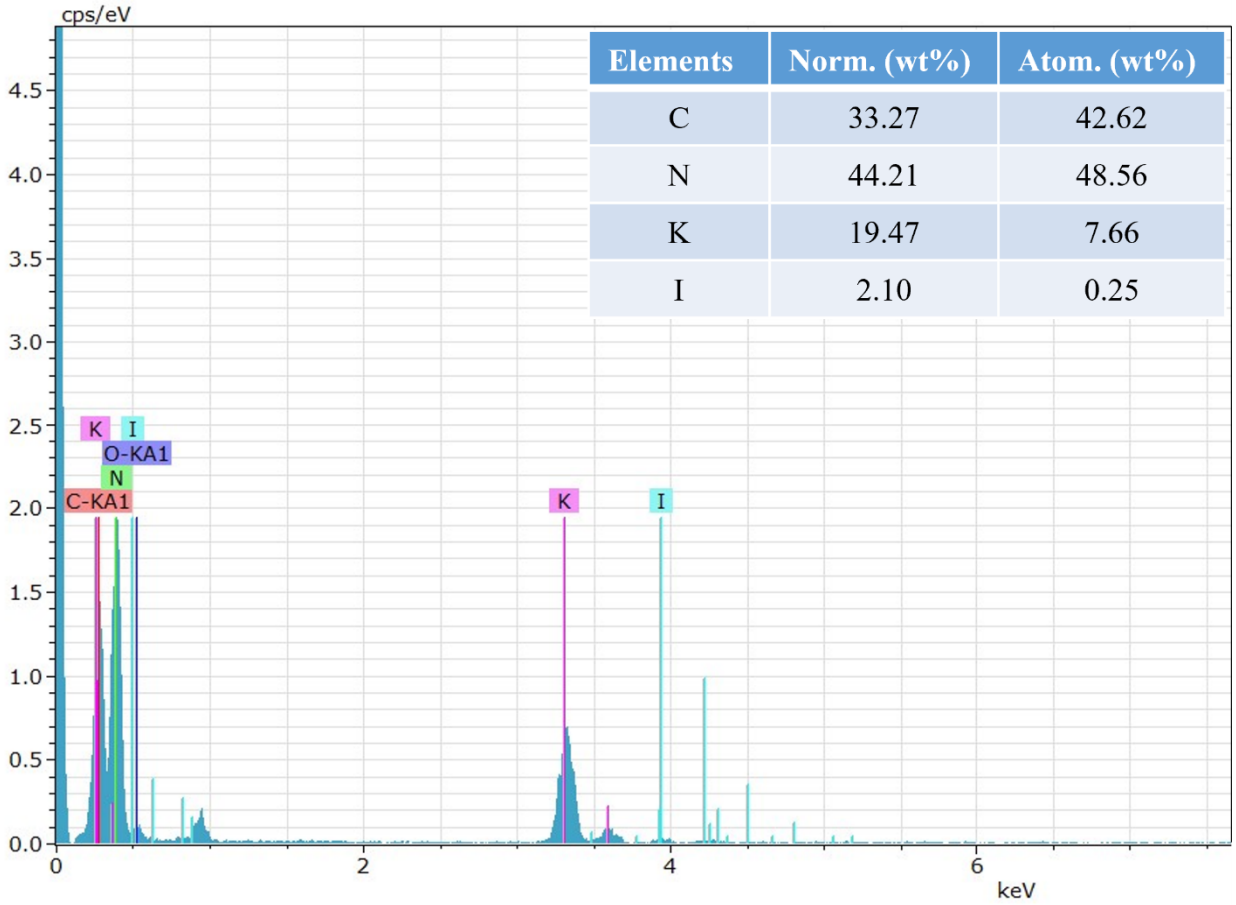

Elements	Norm. (wt%)	Atom. (wt%)
C	33.27	42.62
N	44.21	48.56
K	19.47	7.66
I	2.10	0.25

Fig. S2. EDS spectrum of CN-I_3^-/I^--MV^{2+} 1% composite.

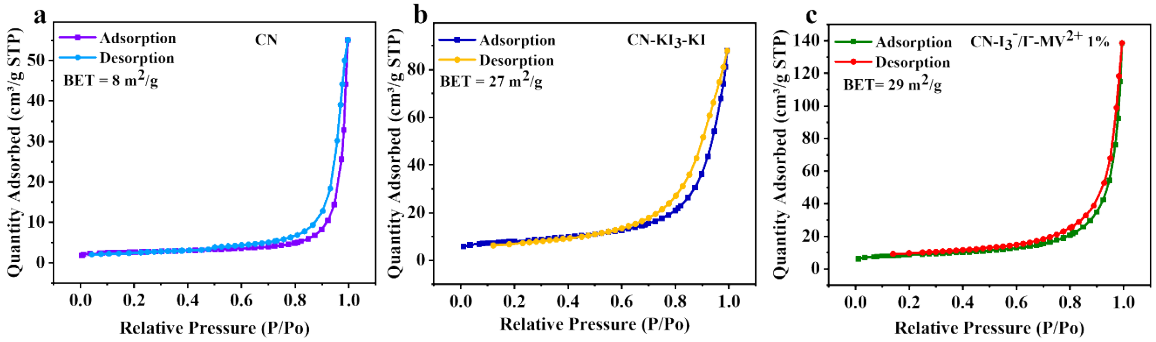

Fig. S3: N_2 adsorption-desorption isotherms of a) CN, b) CN-KI_3-KI, and c) CN-I_3^-/I^--MV^{2+} 1% photocatalysts.

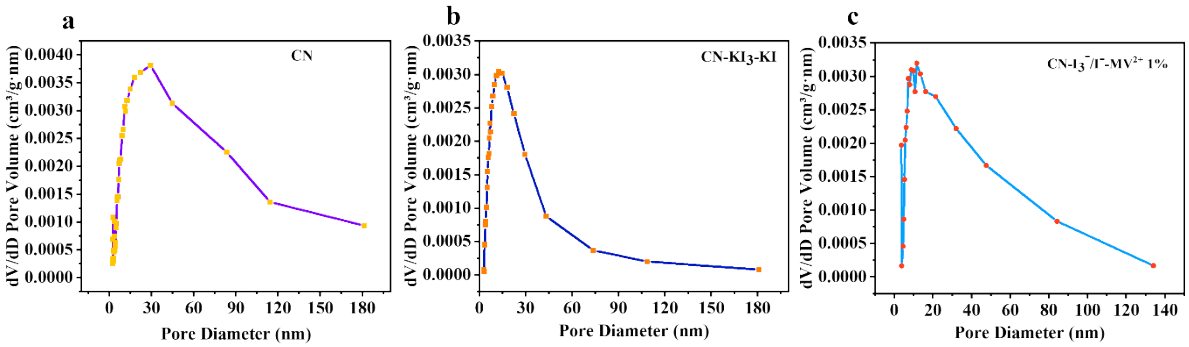

Fig. S4: Pore distribution of a) CN, b) CN-KI_3-KI, and c) CN-I_3^-/I^--MV^{2+} 1% samples.

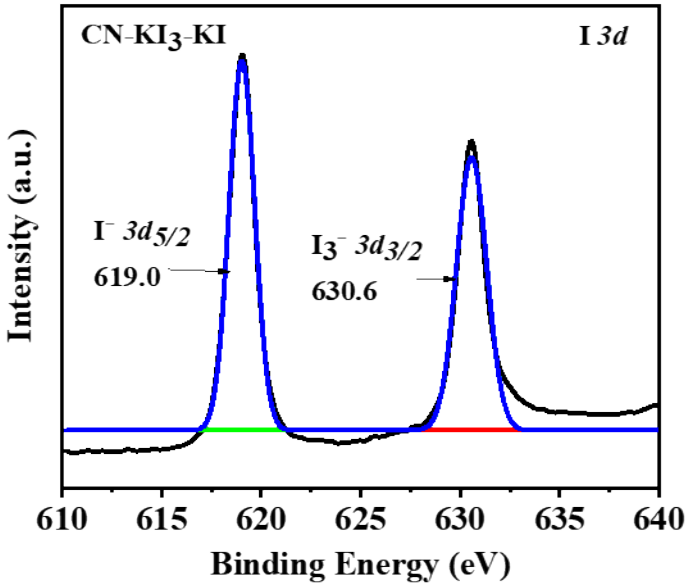

Fig. S5. XPS spectra of I *3d* of CN-KI_3-KI photocatalyst.

Table S1: The position attribution of characteristic peaks in the C *1s* spectrum.

Sample	N-C=N	C-NHx/C≡N	C-C
CN	287.97	286.15	284.66
CN-KI_3-KI	288.04	286.35	284.81
CN-I_3^-/I^--MV^{2+} 1%	288.01	286.25	284.72

Table S2: The position attribution of characteristic peaks in the N *1s* spectrum.

Sample	C-N-H	N-C_3	C-N=C
CN	401.07	399.51	398.45
CN-KI_3-KI	401.87	400.08	398.57
CN-I_3^-/I^--MV^{2+} 1%	400.76	938.70	398.18

Table S3: The position attribution of characteristic peaks in the I *3d* spectrum.

Sample	I^- $3d_{3/2}$	I_3^- $3d_{3/2}$
CN-KI_3-KI	619.01	630.60
CN-I_3^-/I^--MV^{2+} 1%	618.98	630.56

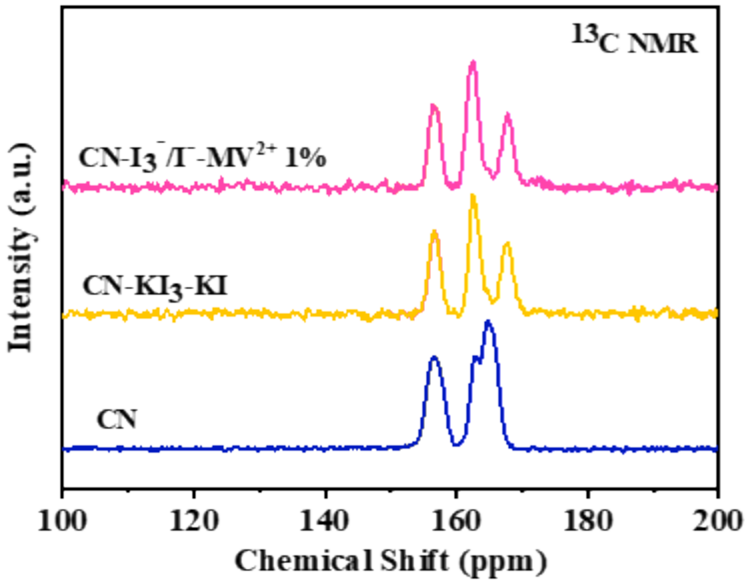

Fig. S6: ^{13}C NMR spectra of CN, CN-KI_3-KI, and CN-I_3^-/I^--MV^{2+} 1% composites.

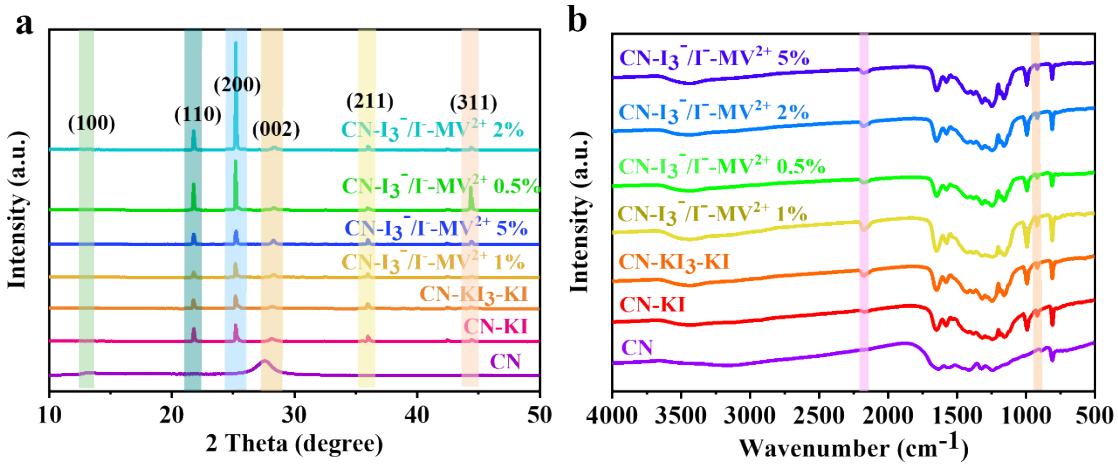

Fig. S7: a) XRD pattern and b) FT-IR spectrum of all synthesized composites.

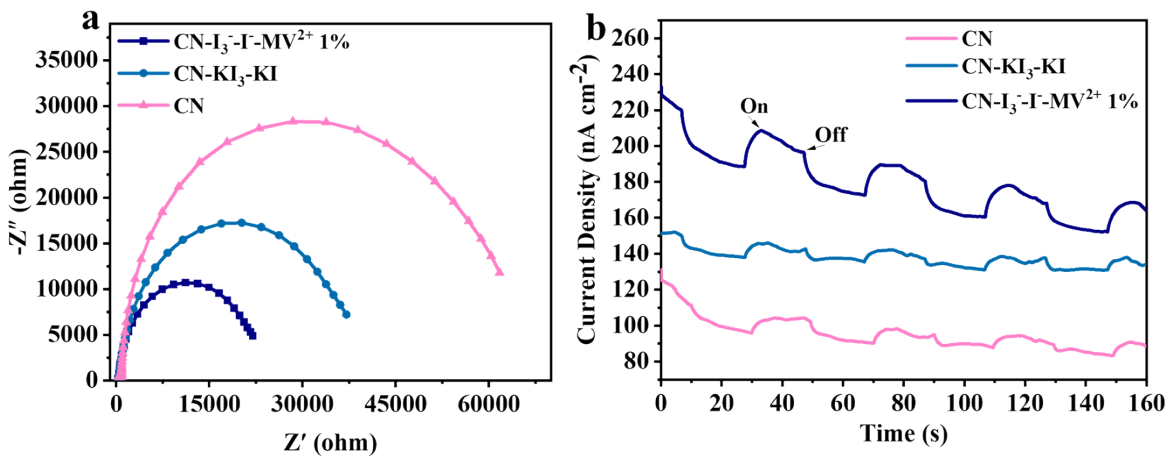

Fig. S8: a) Electrochemical impedance spectra and b) transient photocurrent response spectra of CN, CN-KI_3-KI, and CN-I_3^--I^--MV^{2+} 1% samples.

Table S4. Comparison of our study H_2 evolution results with previously reported other CN photocatalysts.

S.#	Photocatalysts	Reaction conditions	Light source (300 W Xe-lamp)	H_2 evolution rate (μmol h^{-1})	Refs
1.	CN-I_3^-/I^--MV^{2+} 1%	TEOA (10 vol. %), 1 wt% Pt	λ ≥ 420 nm (visible-light)	136.67	This work
2.	K10-g-C_3N_4	TEOA (10 vol. %), 0.5 wt% Pt	λ ≥ 420 nm (visible-light)	102.8	1
3.	CM-K_{12}	TEOA (10 vol. %),1 wt% Pt	λ > 420 nm (visible-light)	127.78	2
4.	CNBS	TEOA (10 vol. %), 1 wt% Pt	150 W Xe-lamp, λ > 420 nm (visible-light)	53.2	3
5.	CN-MV-10	TEOA (10 vol. %), 3 wt% Pt	λ > 420 nm (visible-light)	33.0	4
6.	C_3N_4/CBV^{2+}	TEOA (10 vol. %), 1 wt% Pt	λ ≥ 420 nm (visible-light)	41.57	5
7.	CNUS	TEOA (10 vol. %), 1 wt% Pt	λ ≥ 420 nm (visible-light)	109.3	6
8.	C_3N_{4+x}	TEOA (10 vol. %), 1 wt% Pt	λ ≥ 420 nm (visible-light)	44.28	7
9.	MCN-1	TEOA (10 vol. %), 1 wt% Pt	λ ≥ 420 nm (visible-light)	60.2	8
10.	C_3N_4/CoTPP	TEOA (10 vol. %), 1 wt% Pt	λ ≥ 420 nm (visible-light)	46.93	9
11.	P-TCN	TEOA (10 vol. %), 1 wt% Pt	λ ≥ 420 nm (visible-light)	67	10
12.	MoS_2/g-C_3N_4	TEOA (10 vol. %), 2 wt% Pt	λ ≥ 420 nm (visible-light)	43.38	11
13.	CoP−CN	TEOA (10 vol. %), 2 wt% Pt	λ ≥ 420 nm (visible-light)	51.9	12

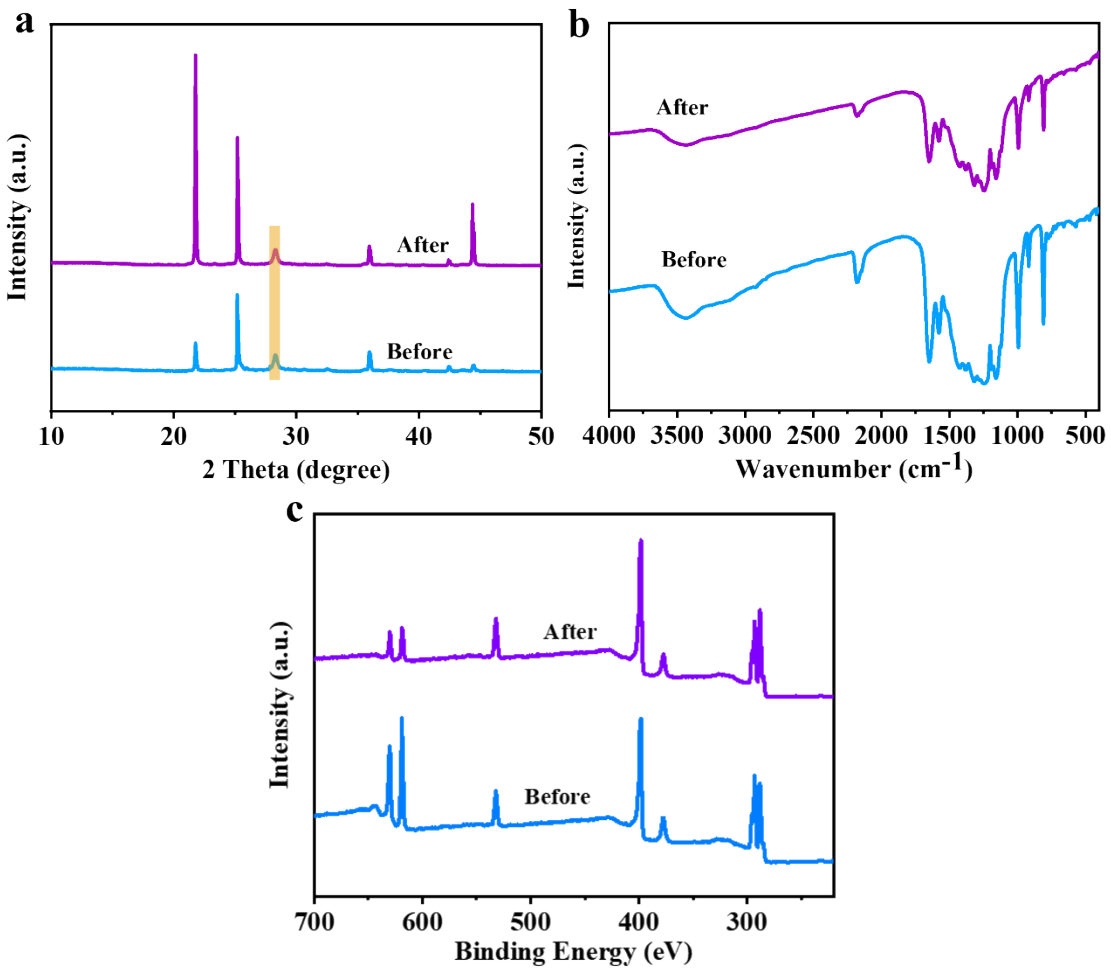

Fig. S9. a) XRD patterns, b) FTIR spectra, and c) XPS survey spectra of CN-I_3^-/I^--MV^{2+} 1% sample before and after the photocatalytic reaction.

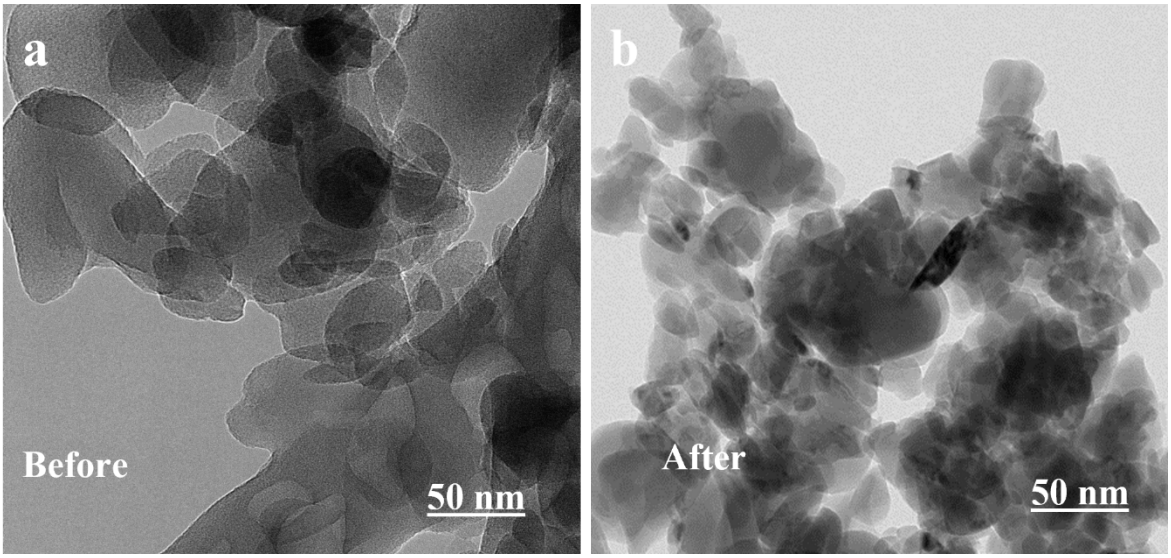

Fig. S10: TEM images of the CN-I_3^-/I^--MV^{2+} 1% sample before and after the photocatalytic reaction.

References

1 M. Wu, J. M. Yan, X. N. Tang, M. Zhao and Q. Jiang, *ChemSusChem*, 2014, **7**, 2654–2658.

2 X. J. Lu, C. Z. Yuan, S. Chen, J. H. Li, I. Ullah, M. Qi and A. W. Xu, *Langmuir*, 2024, **40**, 11067–11077.

3 P. Babu, S. Mohanty, B. Naik and K. Parida, *ACS Appl. Energy Mater.*, 2018, **1**, 5936–5947.

4 F. Bu, R. Yuan, Z. Zhang, J. Wang, J. Liu and Y. C. Yong, *Inorg. Chem. Front.*, 2025, **12**, 801-811.

5 Y. N. Liu, C. C. Shen, N. Jiang, Z. W. Zhao, X. Zhou, S. J. Zhao and A. W. Xu, *ACS Catal.*, 2017, **7**, 8228–8234.

6 Z. Chen, T. Fan, M. Shao, X. Yu, Q. Wu, J. Li, W. Fang and X. Yi, *Appl. Catal. B*, 2019, **242**, 40–50.

7 J. Fang, H. Fan, M. Li and C. Long, *J. Mater. Chem. A Mater.*, 2015, **3**, 13819–13826.

8 Z. F. Huang, J. Song, L. Pan, Z. Wang, X. Zhang, J. J. Zou, W. Mi, X. Zhang and L. Wang, *Nano Energy*, 2015, **12**, 646–656.

9 M. Kombo, L. B. Ma, Y. N. Liu, X. X. Fang, N. Ullah, A. H. Odda and A. W. Xu, *Catal. Sci. Technol.*, 2019, **9**, 2196–2202.

10 S. Guo, Z. Deng, M. Li, B. Jiang, C. Tian, Q. Pan and H. Fu, *Angew. Chem. Int. Ed.*, 2016, **55**, 1830–1834.

11 Y. Liu, X. Xu, J. Zhang, H. Zhang, W. Tian, X. Li, M. O. Tade, H. Sun and S. Wang, *Appl. Catal. B*, 2018, **239**, 334–344.

12 Y. Liu, J. Zhang, X. Li, Z. Yao, L. Zhou, H. Sun and S. Wang, *Energy and Fuels*, 2019, **33**, 11663–11676.